Available online at www.sciencedirect.com
ScienceDirect
Experimental Thermal and Fluid Science 32 (2007) 29–37
Experimental Thermal and Fluid Science
www.elsevier.com/locate/etfs

Smoke leakage through wall openings in a fire

Chan-Wei Wu [a], Ta-Hui Lin [a,*], Chien-Jung Chen [b], Ming-Ju Tsai [b]

[a] Department of Mechanical Engineering, National Cheng Kung University, No. 1, University Road, Tainan 70101, Taiwan, ROC
[b] Architecture and Building Research Institute, Ministry of Interior, Taiwan, ROC

Received 20 June 2006; received in revised form 19 December 2006; accepted 12 January 2007

Abstract

This study developed a full-scale smoke-barrier system and established a testing procedure to investigate wall openings of various geometric shapes, which may be passageway for cables and pipes and are usually of irregular shapes, for different pressure differences and temperatures. In addition, a simple analytical model was developed to correlate the experiment data. The results showed that the smoke leakage rate was dependent on several factors, including pressure difference, gas temperature, geometric shape and area of opening. The rate of smoke leakage was proportional to the square root of the pressure difference or to the reciprocal of the square root of the upstream gas temperature. An opening of higher perimeter-to-area ratio had higher resistance against smoke flow and thus allowed smaller rate of smoke leakage. Finally, a geometric loss factor was assigned to the tested wall opening to indicate its smoke leakage characteristics. In the study, the capability of the testing device and the application of the testing procedure were verified to be suitable for the fire tests of more complicate objects, such as smoke barriers or doors, in the future.

Keywords: Wall opening; Smoke leakage rate; Smoke-barrier testing device

1. Introduction

Smoke contents and its movement are among the basic elements for the characterization of a fire situation. The combustion conditions, e.g., flaming, pyrolysis, and smoldering, affect the amount and properties of the smoke. In an ordinary fire, personal injury does not substantially result from the scorching of the heat but rather from the choking or poisoning of the smoke. As the personal incomes and the living quality are improved, interior decorations pile up and more smoke-producing materials, such as PVC boards, plastics, fireproof boards and planks are used. As these inflammable materials burn, plenty of smoke, irritant toxic gases and carbon monoxide would easily be produced. Thus, smoke control and smoke barrier have become increasingly important. Recently, some regulations related to smoke leakage, such as ISO 5925/1 [1], ISO 5925/2 [2] and UL 1784 [3] have been established.

In ISO 5925, it mainly evaluates the performance of door and shutter assemblies intended to act as barriers of smoke in a fire under different pressure variations (5–100 Pa) and different temperature modes (ambient temperature, 200 °C and an undefined high temperature) to measure the smoke leakage. The standard of UL 1784 describes the investigation of air leakage through door assemblies installed in wall openings where air leakage is to be controlled. And the purpose of the test is to determine only the resistance of a door assembly, in the closed position, to air leakage resulting from a specified air pressure difference applied across the surface of the entire door assembly. Basically, the testing methods of ISO 5925 and UL 1784 are very similar.

From the early 1980s, researchers started to do experiments on smoke dampers. Smoke dampers can be either passive or active. In passive smoke management systems, smoke dampers are intended for the inhibition of smoke passage under such forces as buoyancy, stack effect, and

* Corresponding author. Tel.: +886 6 2752525x62167; fax: +886 6 2352973.
E-mail address: thlin@mail.ncku.edu.tw (T.-H. Lin).

0894-1777/$ - see front matter © 2007 Elsevier Inc. All rights reserved.
doi:10.1016/j.expthermflusci.2007.01.004

Nomenclature

A	area, m^2
D	hydraulic diameter of the opening ($4 \times$ cross-sectional area/wetted perimeter), m
F_R	friction force, N
K_L	geometric loss factor, dimensionless
$\dot{m}$	mass rate of smoke leakage, kg/s
P	pressure, Pa
ΔP	pressure difference across the specimen, Pa
$\dot{Q}$	volumetric smoke leakage rate, m^3/s
Re	Reynolds number, $\frac{\rho_o V_o D_h}{\mu_o}$
T	temperature, °C
TC_1–TC_9	measured temperatures in the pressure chamber, °C
TC'_1–TC'_9	measured temperatures in the gastight chamber, °C
T_{in}	temperature of the inlet hot gas into the pressure chamber, °C
T_{out}	downstream temperature of the leaking smoke, which is measured right before the flow rate measuring device, °C
V	velocity of smoke, m/s

Greeks

β	density ratio, dimensionless
ρ	smoke density, kg/m^3
ρ_s	smoke density at the flow measuring point, kg/m^3

Subscripts

o	opening
1	upstream of the pressure chamber
2	downstream of the gastight chamber

wind. Dampers with low leakage characteristics are advantageous for passive applications. In active smoke control systems, smoke dampers are used to control the passage of air which may or may not contain smoke [4]. Cooper [5] identified relevant parameters on the smoke leakage characteristics of door assemblies. He suggested a series of door assembly test methods based on a review of the availability and development status of existing and potential test method candidates. Furthermore, the concept of smoke compartmentation and the importance of cross-door pressure differential in accessing the performance of door assemblies in a fire-generated environment were introduced and developed.

With the progress of fire researches, the knowledge of smoke propagation in a fire has been further understood. Klote [6,7] mentioned that smoke propagation in the scene of a fire was related to many factors such as the temperature, states of the doors and windows, strength of the wind, position of the smoke-barrier device, chimney effect and design of air-conditioner and so forth. Thus, the function and the applicability of a smoke-barrier device in a building cannot be identified with just one test method or one leakage standard. Sudo et al. [8] followed ISO 5925/1 and conducted a leakage test for fire doors. They pointed out that the performance of a smoke-barrier was in relation to the position of the installation, as well as the intensity of heat source and pressure differences. Therefore, the smoke-barrier device should be provided with temperature and pressure-difference adjustments. Their results showed, as expected, that larger leakage area would let out more smoke. When the heating temperature rose to 400 °C and the pressure differences fell below 100 Pa, the smoke leakage would decrease dramatically.

Based on the process provided in ISO 5925/1, Sheppard and Aittaniemi [9] utilized two kinds of fire damper, a fire stop and seven fire doors to test the smoke leakage. The specimen was first heated to about 180 °C to measure the distortion and after the specimen cooled down they proceeded with the smoke leakage test. The pressure differences were set up from 5 to 100 Pa to analyze the relation between the pressure difference and the smoke leakage at the ambient temperature. In general, as the pressure differences increased, the smoke leakage increased.

Kazuki [10] investigated the heat insulation characteristic and smoke-blockage performance of a window, in a simulated fire. Their result showed that, below a certain temperature, the amount of smoke leakage depended only on the clearance between the frame and the window. When the temperature exceeded some higher values, however, the major factors which would affect leakage characteristics became the crevice or breakup of the window.

Sudo et al. [11] examined the smoke-barrier performance of fireproof dampers in high temperature environments and investigated the influences of pressure differences and heating temperature on smoke leakage. When temperature was below 400 °C, the characteristics of smoke leakage was nearly equal to those at room temperature. When the heating temperature was raised over 600 °C, however, the synthetic rubber used as airtight materials were burnt and deformed; as a result, large amount of smoke appeared owing to generation of the gap. It was also found that heating position (indoor or outdoor) has no effects on smoke leakage.

Another research [12] used sheet-metal damper to study the influences of effective open-area on smoke-barrier performance. The results indicated that the amount of smoke leakage for each testing specimen was almost linearly proportion to the increase of pressure. Owing to the known performance of the sheet-metal damper as smoke-barrier, the clearance between pipe-wall and damper was inferred

to be the most important factor which caused leakage as pressure difference increased.

In modern multi-storey buildings, there are wall openings for the passage of air conditioning ducts, pipes, and cables. Together with doors and windows, they form a link between the inside of a room to the outside environments. As a fire occurs inside or outside the room, the combustion gases and smoke would flow through the openings and cause personal or property damage. Thus, the principal factors which control the movement of the combustion gases and smoke through these openings deserve our attention. Full-scale testing of smoke leakage in a high-temperature environment simulating a real fire has been little studied. In view of this, the present study first established a full-scale smoke-barrier testing device and then investigated wall openings of various geometric shapes, which may be passageway for cables and pipes and are usually of irregular shapes, for different pressure differences and temperatures. This study can aid in the understanding of the principles governing smoke flow through irregular wall openings in a fire.

2. Experimental apparatus and methods

A smoke-barrier system had been designed and constructed in this study, as shown in Fig. 1. It consisted of a refractory wall/door testing furnace (Fig. 1b) and a smoke-barrier device (Fig. 1c). The smoke-barrier system could be used to simulate and examine the smoke behavior though openings (vents or holes), door and shutter assemblies in a building fire.

2.1. Refractory wall/door testing furnace

A refractory wall/door testing furnace was used to provide high-temperature combustion gases to the

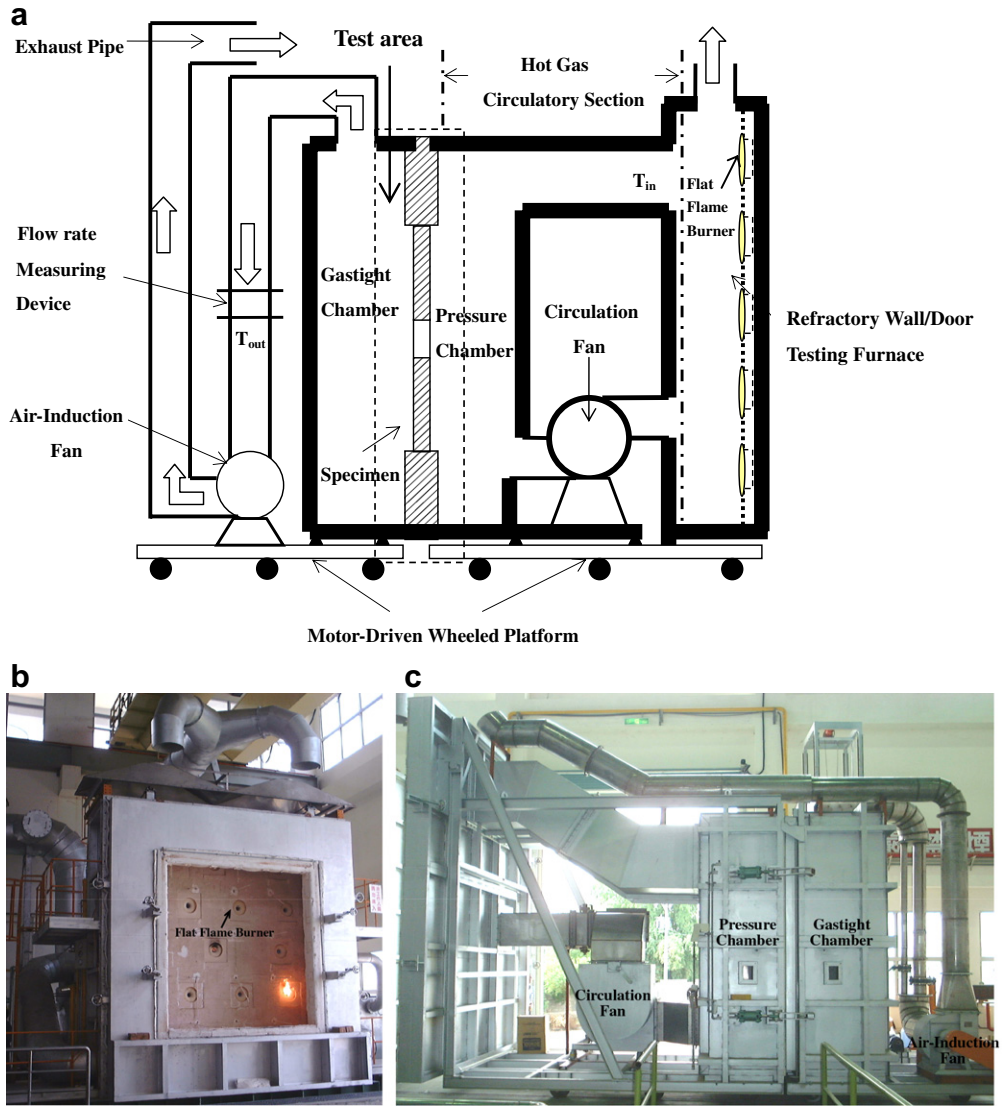

Fig. 1. The scheme and pictures of the smoke-barrier system: (a) smoke-barrier system; (b) refractory wall/door testing furnace; and (c) smoke-barrier testing device.

smoke-barrier testing device for the simulation of smoke flow in a fire. The standards of construction and the functions of the furnace were in accordance with ISO 834, CNS 11227 and ISO 3008. The inner and outer dimensions of the furnace were $430W \times 450H \times 100L$ (cm) and $500W \times 520H \times 140L$ (cm), respectively. Steel structures were used on the exterior of the furnace, test frame, air supply device, exhaust duct and hood. The surfaces inside the furnace were covered with fireproof ceramic-fiber materials capable of enduring a temperature over 1400 °C. The fuel used was LPG and the burning system contained flat flame burners, which were all equipped with UV flame sensors to monitor the flame state. The available testing area, which was directly exposed to the furnace fire, and the maximal testing duration were $300W \times 300H$ (cm) and 4 h, respectively.

2.2. Smoke-barrier testing device

The smoke-barrier testing device could be divided into five sections, such as hot-gas circulatory section, gastight chamber, temperature/pressure feedback system, motor-driven wheeled platform and the specimen. The whole configuration is sketched in Fig. 1a. The airtight hot-gas circulatory section contained a pressure chamber and a circulation fan (800 °C, 240 m^3/min, 50 mmAq). The circulation fan blew the hot gases from the refractory furnace, to form a high-temperature and constant-pressure environment in the upstream of the test specimen to simulate the smoke distribution of an actual fire. The gastight chamber was composed of an air-induction fan (300 °C, 100 m^3/min, 50 mmAq), exhaust pipes and a flow meter (orifice type, 4–20 mA output). The air-induction fan controlled the downstream pressure of the test specimen so as to establish a specified pressure difference across the specimen and then the flow rate of the smoke leakage could be measured. The temperature and pressure feedback system included K-type thermocouples (the accuracy was 1000 ± 4.73 °C), pressure transducers, data management systems and control panels. The specimen embedded in the testing frame, which was set up between the pressure chamber and the gastight chamber, could be of various types such as wall openings, fire dampers, fireproof wood doors and steel doors, etc. In this study, wall-opening specimens of different geometric shapes were used for examining their smoke leakage characteristics.

2.3. Experimental methods

The hot combustion gas in the refractory wall/door testing furnace was drawn into the pressure chamber by the circulation fan; and the temperature in the chamber was controlled at certain nominal values (100, 200, 300, 400, or 500 °C) to simulate various fire intensities. Fig. 2a and b indicate locations of 18 thermocouples and the wall-opening specimen on the testing frame, viewing from the pressure-chamber side and gastight chamber side, respectively. All thermocouples stayed 10 cm away from the surface of the testing frame. The testing frame, which was set up between the pressure chamber and the gastight chamber, was a 3 m × 3 m concrete wall with a 1 m × 1 m steel plate of thickness 5 mm at the center. And the steel plate installed a wall opening of a certain area and a certain geometric shape, which was used for smoke leakage testing in this study. Thermocouples TC_1–TC_9 measured the temperature distribution of the pressure chamber side (upstream high-temperature side) of the specimen; and thermocouples TC_1'–TC_9' measured the temperature distribution of the gastight chamber side (downstream low-temperature side) of the specimen.

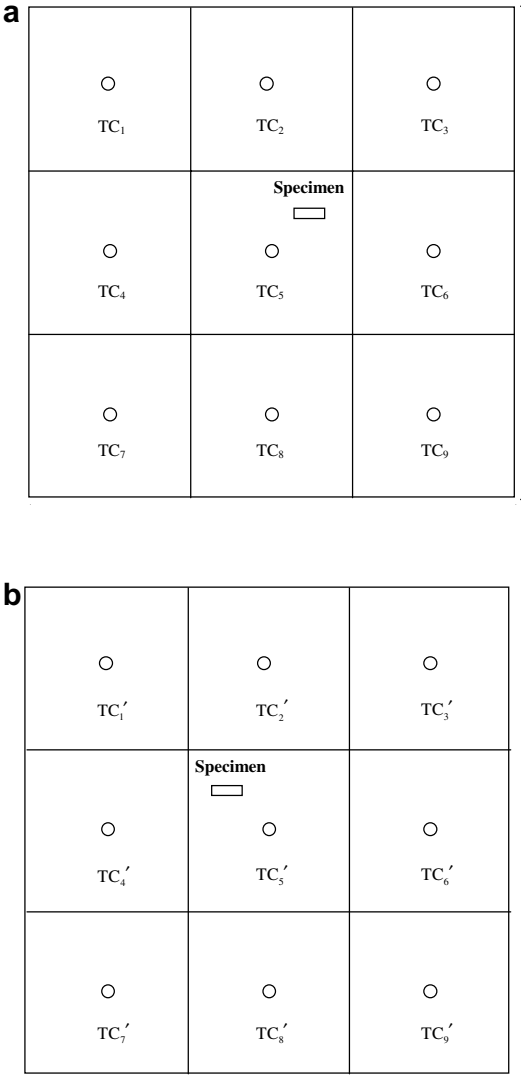

Fig. 2. Locations of thermocouples and the wall-opening specimen on the testing frame: (a) pressure-chamber side and (b) gastight-chamber side.

In the present experiment, three openings with different geometric shapes of rectangular, square and circular were used. The pressure differences were controlled at 30, 50, 100, 150, 200, 250 or 300 Pa across the specimen by changing the capacity of the air-induction fan. The temperature in the pressure chamber was controlled and maintained

with a 100 °C stepwise increment from the room temperature to 500 °C. The temperature steps specified here were only nominal. By controlling the burning intensity of the burners in the refractory furnace together with the hot gas recirculation, the real temperature in the pressure chamber gradually approached to the setting value. The real temperature reached in each step was not exactly the same as the setting value, but it remained constant and steady for a period of time in which the pressure differences were generated and the smoke leakage rates were also measured at the same time. Therefore, if one followed the same controlling strategy to obtain the same real temperature, the repeatability of measuring the smoke leakage rate was acceptable with error less than 5%. The above-mentioned experimental conditions covered the range of temperatures and pressure differences commonly observed in a domestic fire.

3. Results and discussions

3.1. Room-temperature testing

Fig. 3 shows the rate of smoke leakage through different leakage areas of square opening at ambient temperature as a function of pressure difference. In the figure, A_o and $\dot{Q}$ respectively indicate the leakage area of square opening and the volumetric smoke leakage rate. T_1 and ΔP represent the average operating temperature in the pressure chamber and the pressure difference across the specimen, respectively. First we notice that as the leakage area was equal to 0 cm^2, for all pressure differences, the leakage rate of the system approached 0 m^3/min. This ensured the air tightness of the gastight chamber.

The volumetric smoke leakage rate increased as either the leakage area or the pressure difference increased. The volumetric flow rate of smoke leakage was seen to vary proportionally with the leakage area for a fixed pressure difference or with the square root of pressure difference for a fixed leakage area. For example, as pressure difference increased from 50 Pa to 300 Pa for a leakage area of 30 cm^2, the volumetric flow rate of leakage rate would increase from 1.2 to 3.2 m^3/min. These relations can be easily explained by basic principles for constant-temperature incompressible flows in fluid mechanics. After viewing the room-temperature test result, performance and control of the smoke-barrier system were found adequate for further executing high-temperature leakage tests in which a fixed 30 cm^2 leakage area was chosen as the opening area of the specimen.

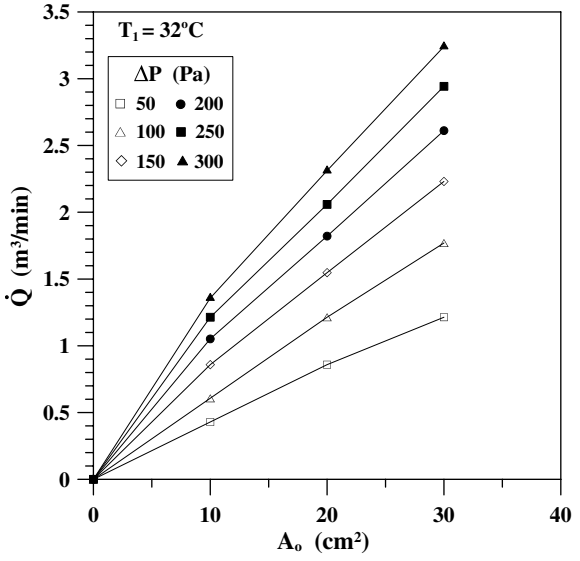

Fig. 3. Variations of smoke leakage rate with A_o under various pressure differences at ambient temperature for a square wall opening.

3.2. Smoke leakage at high temperatures

During the high-temperature smoke leakage test for various pressure differences across the specimen, the temperature distribution in the pressure chamber should be maintained uniform and constant in the data recording period at each testing condition. Thus, stepwise temperature control in the refractory furnace was adopted for the experiments. Five temperature steps (100, 200, 300, 400 and 500 °C) were assigned, and for each temperature, seven pressure differences (30, 50, 100, 150, 200, 250 and 300 Pa) were applied across the specimen to measure the rate of smoke leakage. The temperature steps specified here were only nominal. All measurements and corresponding calculations were based on real time data output.

Temperature distributions in both sides of the testing frame embedded with a rectangular shape of opening are shown in Fig. 4 as an example to illustrate the temperature variations in the experiment. Fig. 4a shows variations of temperature distribution in the pressure chamber. The symbol T_{in}, taken inside the refractory furnace, represents the temperature of the inlet hot gas into the pressure chamber. TC_1–TC_9 indicate the temperatures of the nine thermocouples on the pressure-chamber side of the specimen; and TC_{avg} is the average of TC_1–TC_9. The inlet temperature T_{in} was higher than TC_1–TC_9 and TC_{avg} in the pressure chamber because of the heat loss during the circulation of the hot gas. The curves of temperature variation for nine thermocouples (TC_1–TC_9) were quite close, indicating a uniform temperature distribution on the pressure-chamber side at any instant in the experiment. The smoke leakage measurements were performed during the time period when the temperature reached a step and stayed nearly constant. The uniformity of temperature distribution on the pressure-chamber side at any instant was mostly critical and important in this study.

Fig. 4b represents the temperature distribution on the gastight-chamber side of the specimen. T_{out} is the downstream temperature of the leaking smoke, which was measured right before the flow rate measuring device. TC'_1–TC'_9 indicate the temperatures of the nine thermocouples on the gastight-chamber side of the specimen; and TC'_{avg} is their

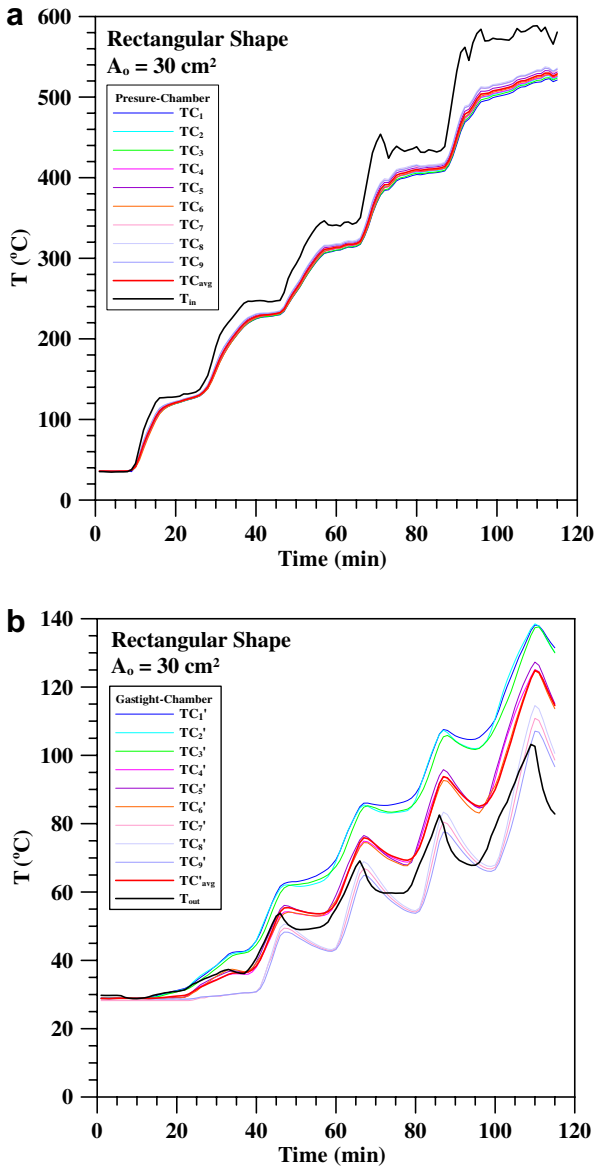

Fig. 4. Temperature distributions on both sides of the specimen: (a) pressure-chamber side and (b) gastight-chamber side.

average. It could be clearly seen that there were several valleys which exactly corresponded to the temperature steps shown in Fig. 4a. As TC_{avg} reached closely to the assigned value and stayed nearly constant for a given temperature step as shown in Fig. 4a, the induction fan was started to generate various pressure differences in a stepwise fashion. With increasing the pressure difference in the process, the hot gas was drawn from the pressure chamber into the gastight chamber resulting in an increase of temperature in the gastight chamber. The increasing temperature reached a local maximum shown in Fig. 4b until the leakage test was done with shutting down the induction fan. Being forward to the next temperature step, the temperatures (TC_1–TC_9) of the pressure chamber increased, while the temperatures (TC'_1–TC'_9) of the gastight chamber gradually decreased because of the heat loss through the gastight chamber. The oscillatory behavior of temperature variation described above could be regarded as a necessary result owing to the operation strategy in this study.

As can be seen in Fig. 4b, the temperatures of TC'_1–TC'_3 were the highest and TC'_7–TC'_9 were the lowest. The hot gases through the opening flowed upward because the outgoing pipe was positioned on top; and therefore, the upper region of the gastight chamber had higher temperatures than the lower region. Since the temperatures of TC'_1–TC'_3 were almost the same, similar observation for TC'_4–TC'_6, it is worth to mention that the temperature distribution was uniform along the same height in the upper and middle region of the gastight chamber.

In this study, three specimens of area 30 cm^2 with geometric shapes of rectangular (10 cm × 3 cm), square (5.48 cm × 5.48 cm), and circular (6.18 cm in diameter) were tested for their high-temperature smoke leakage rates. To facilitate comparison, the measured volumetric smoke leakage rates were corrected to mass smoke leakage rates, which is shown as follows:

$$\dot{m} = \rho_s \times \dot{Q}, \tag{1}$$

where $\dot{m}$ is the mass smoke leakage rate (kg/min); $\dot{Q}$ is the measured volumetric flow rate (m^3/min); and ρ_s is the smoke density (kg/m^3) at the flow measuring point obtained from the ideal gas law by using the local temperature and pressure.

Fig. 5 shows the mass flow rate of smoke leakage $\dot{m}$ as a function of pressure-chamber temperature T_1 (corresponding to the measured TC_{avg}) for various pressure differences ΔP for the three specimens. In the experiment, as T_1 increased from 30 °C to 500 °C, the mass smoke leakage rate decreased gradually and this decreasing trend was more apparent for higher pressure differences. Openings of different geometric shape had similar temperature dependency. It is noteworthy that the mass smoke leakage rate had its largest value at room temperature. In Fig. 5, the rate of smoke leakage $\dot{m}$ was also seen to increase as the pressure difference increased. Before more discussions on the experimental data, we shall attempt to use a mathematical model to identify the parameters governing the leakage rate.

3.3. Smoke leakage characteristics analysis

Sketched in Fig. 6 is the schematic of a smoke-leaking wall opening which is subjected to a high temperature gas on the upstream side. The symbols A, P, ρ, V, and T represent local area of the opening, pressure, density, velocity and temperature of the gas flow. The variables corresponding to the pressure chamber, the gastight chamber, and the opening are designated by subscripts 1, 2, and o, respectively. Based on Fig. 4, it was found that at any instant, the temperature distribution was entirely uniform in the pressure chamber, and was also uniform along the same height in the upper and middle region of the gastight chamber. Since the area of the specimen was relatively small in comparing with the total area of the testing chamber, it is reasonable

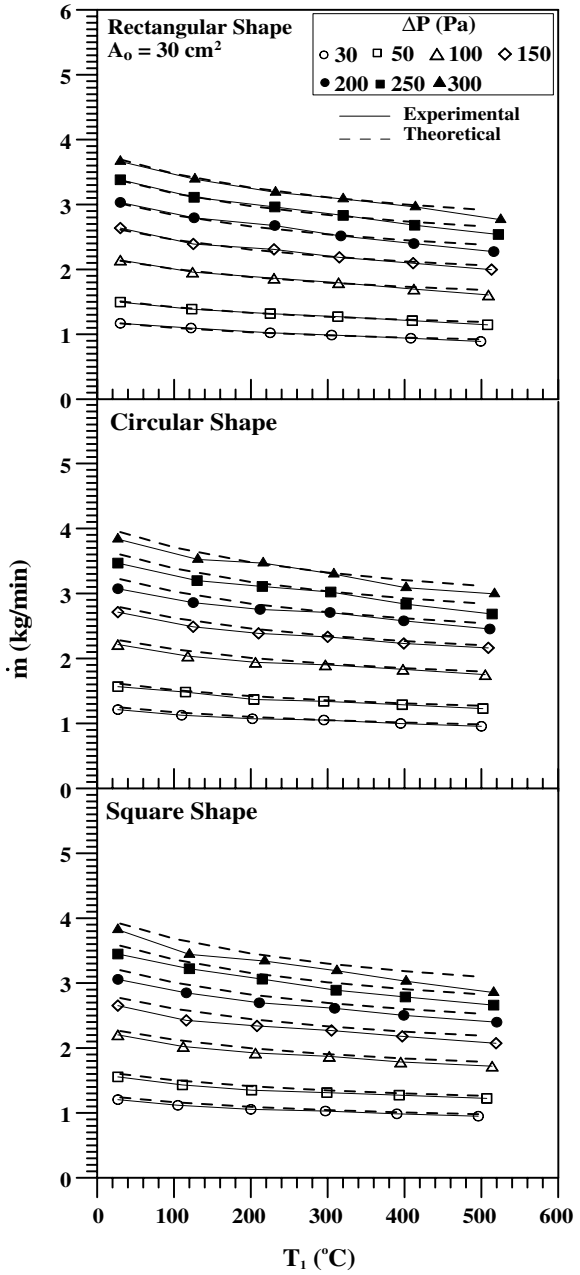

Fig. 5. Variations of smoke leakage rate with pressure-chamber temperature and pressure differences for various wall openings.

to focus our attention to the neighborhood of the specimen and neglect the height influence by using one-dimensional flow assumption in our analysis. Taking a mass and momentum balance between the upstream and downstream sides of the opening, we obtain the following equations:

$$\text{Continuity equation:}\quad \dot{m} = \rho_1 A_1 V_1 = \rho_2 A_2 V_2 = \rho_o A_o V_o, \tag{2}$$

$$\text{Momentum equation:}\quad P_1 - P_2 - \frac{F_R}{A_o} = \rho_2 V_2^2 - \rho_1 V_1^2. \tag{3}$$

In the momentum equation, F_R is regarded as a momentum loss from the friction of the opening and can be

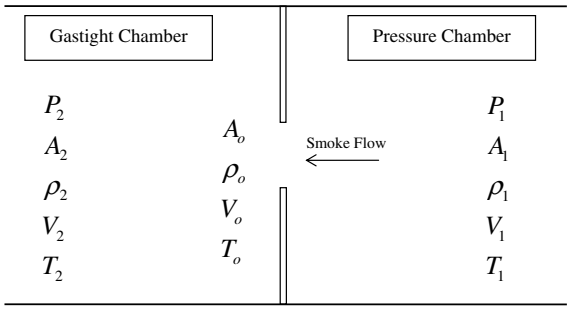

Fig. 6. An analytical model for the one-dimensional smoke flow.

written as $F_R = A_o K_L \left(\frac{\rho_o V_o^2}{2}\right)$, where K_L is the geometric friction factor. Considering $A_1 \approx A_2$, the momentum equation can then be rearranged as

$$P_1 - P_2 - K_L \frac{\rho_o V_o^2}{2} = \frac{\rho_o^2 V_o^2 A_o^2}{\rho_1 A_1^2}\left(\frac{\rho_1}{\rho_2} - 1\right). \tag{4}$$

By assuming the density at the opening as a certain multiple of ρ_1, i.e., $\rho_o = \beta\rho_1$, where $\beta \geqslant 1$, and then the velocity V_o can be derived as

$$V_o = (\beta\rho_1)^{-\frac{1}{2}}(P_1 - P_2)^{\frac{1}{2}}\left[\frac{K_L}{2} + \frac{\beta A_o^2}{A_1^2}\left(\frac{\rho_1}{\rho_2} - 1\right)\right]^{-\frac{1}{2}}. \tag{5}$$

The mass flow rate is further expressed by

$$\dot{m} = A_o(\beta\rho_1)^{\frac{1}{2}}(P_1 - P_2)^{\frac{1}{2}}\left[\frac{K_L}{2} + \frac{\beta A_o^2}{A_1^2}\left(\frac{\rho_1}{\rho_2} - 1\right)\right]^{-\frac{1}{2}}. \tag{6}$$

From Eq. (6), it can be seen that there are four major factors influencing the mass flow rate, namely, A, ρ, ΔP, and K_L. If the opening is small compared with cross section A_1, i.e. $A_1 \gg A_o$, Eq. (6) can be reduced to the following equation:

$$\dot{m} = \sqrt{2} A_o \beta^{\frac{1}{2}} \rho_1^{\frac{1}{2}} K_L^{-\frac{1}{2}} \Delta P^{\frac{1}{2}}, \tag{7}$$

where ρ_1 is inversely proportional to T_1, if the ideal gas law is assumed. Eq. (7) shows that $\dot{m}$ varies with the $\frac{1}{2}$th power of ΔP or ρ_1 (or the negative $\frac{1}{2}$th power of T_1). In this equation, A_o is taken as constant because the thermal expansion coefficients of steel and concrete are small. K_L is a function of the geometry of the opening and the Reynolds number of the flow. Since the narrow range of Reynolds number involved in the experiment, K_L varied slightly with the Reynolds number for a given opening. For simplicity in the calculation, the K_L in Eq. (7) may be treated as a constant taken by an average value from the experiment. Based on the ideal gas assumption, the β in Eq. (7) showing the ratio of ρ_o and ρ_1 is proportional to the ratio of T_1 and T_o. From the interpolation between T_1 (the measured TC_{avg}) and T_2 (the measured TC'_5) in the experiment, T_o can be determined and further coupled with T_1 to achieve a simple correlation equation $\beta = 1.3 \times 10^{-3} T_1 + 0.992$ ($T_1 \geqslant 30$ °C) being used in Eq. (7) for calculations.

With the above-mentioned strategy, the theoretical relations of mass flow rate ($\dot{m}$) to pressure difference (ΔP) or

temperature (T) are plotted in Fig. 5 as dashed lines for comparison. In Fig. 5, the analytical model predicts the temperature dependency of the mass smoke leakage rate correctly. In previous studies, the decrease of mass smoke leakage rate for higher temperature was usually attributed to the thermal expansion of the specimen. But the thermal expansion coefficient of steel was so small (in the order of 10^{-5} m/m), this reasoning is questionable. According to the Eq. (7), it could be known that the mass smoke leakage rate is directly proportional to the density $\rho_1^{\frac{1}{2}}$ which is equivalent to $T_1^{-\frac{1}{2}}$. As the temperature T_1 increases, the inlet smoke density would reduce. Thus the mass smoke leakage rate would decrease with $-\frac{1}{2}$th power of T_1; and the thermal expansion effect would be regarded as an insignificant factor.

3.4. Smoke leakage influenced by geometrical shapes

Fig. 7 describes the differences of mass smoke leakage rate for different geometric openings under different pressure differences and temperatures. For all cases, the flow rates of the circular and square openings were closer to each other than to the rectangular opening; and they had higher leakage rate than the rectangular opening. Take pressure difference $\Delta P = 200$ Pa and temperature T_1 from 30 °C to 500 °C for example, the mass smoke leakage rates of rectangular and circular openings were from 3.03 to 2.27 and 3.07 to 2.45 kg/min, respectively. The increment of smoke leakage for circular openings comparing to rectangular opening was about 1–8%. The reason is certainly that the geometric loss factor K_L for the rectangular opening was larger than that of square opening. The higher value of K_L of the rectangular opening came from its higher perimeter-to-area ratio than the other two openings.

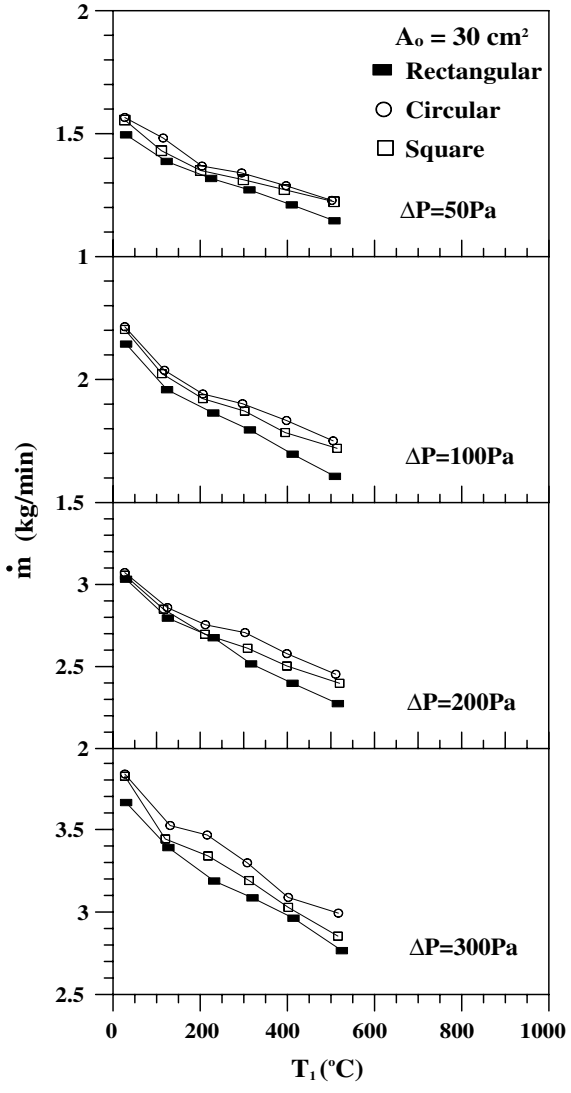

Fig. 7. Variations of smoke leakage rate with T_1 and ΔP for various wall openings.

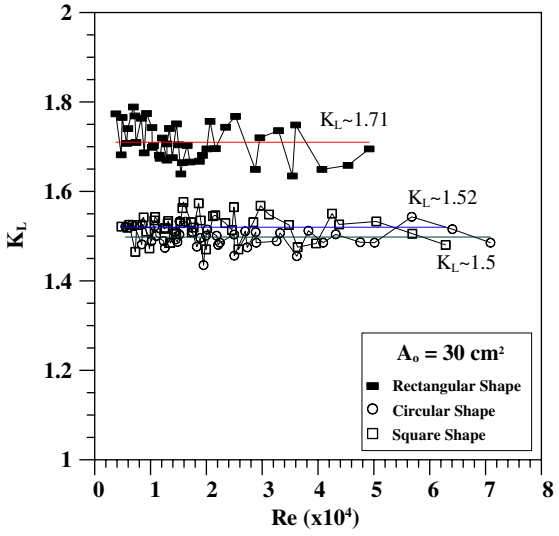

Fig. 8. The geometric loss factor as a function of Reynolds number for various wall openings.

Fig. 8 shows a correlation of K_L with various Reynolds numbers (Re) for each geometric shape. K_L was calculated from the formula of $\frac{2\Delta P}{\rho_o V_o^2}$. The Reynolds number was defined at the opening as $\frac{\rho_o V_o D_h}{\mu_o}$, where D_h was the hydraulic diameter of the opening. ρ_o and μ_o were functions of T_o which was determined by the interpolation between T_1 (the measured TC_{avg}) and T_2 (the measured TC'_5). V_o was simply $\frac{\dot{Q}}{A_o}$. From Fig. 8, it is found that K_L was nearly independent of Reynolds number (Re) for the same opening, and was just a function of the geometric shape. For the rectangular opening, the average K_L was about 1.71; and for the circular and square openings, they were about 1.5 and 1.52. A higher K_L indicated a smaller leakage rate if all other conditions were fixed.

4. Conclusion

This study developed a large-scale smoke-barrier testing device and established a testing procedure to investigate the rate of smoke leakage for a horizontal wall opening under different pressure differences and temperatures, as might be encountered in an actual fire. An analytical model for the

dependence of smoke leakage rate on pressure difference and temperature was also presented and compared with the experiment findings. The conclusions are summarized as follows:

(1) The smoke leakage rate is dependent on several factors including pressure difference, gas temperature, geometric shape and area of opening.
(2) The rate of smoke leakage ($\dot{m}$) is proportional to the square root of the pressure difference (ΔP) or is inversely proportional to the square root of the upstream temperature (T_1).
(3) An opening of higher perimeter-to-area ratio has higher resistance against the smoke flow and thus results in smaller rate of smoke leakage.
(4) The geometric loss factor (K_L) of the opening varies slightly for the narrow range of Reynolds number encountered in this study.

In this study, the capability of the testing device and the application of the testing procedure were finally verified to be suitable for the fire tests of more complicate objects, such as smoke barriers or doors, in the future.

References

[1] ISO 5925/1, Fire tests – evaluation of performance of smoke control assemblies – part1: ambient temperature test, International Organization for Standardization, 1981.
[2] ISO 5925/2, Fire tests – smoke control door and shutter assemblies – part2: commentary on test method and test data application, International Organization for Standardization, 1997.
[3] UL 1784, Air leakage tests of door assemblies, Underwriters Laboratories Inc. Standard for Safety, 2001.
[4] R.M. Plettner, What is a smoke damper? a summary of UL standard 555s – leakage-rated dampers for use in smoke control systems, ASHRAE Transactions 90 (1984) 655–664.
[5] L.Y. Cooper, Need and Availability of Test Methods for Measuring the Smoke Leakage Characteristics of Door assemblies, ASTM Special Technical Publication, 1985, pp. 310–329.
[6] J.H. Klote, Design of smoke control systems for areas of refuge, ASHRAE Transactions 99 (2) (1993) 793–807.
[7] J.H. Klote, An overview of smoke control research, ASHRAE Transactions: Symposia 101 (1) (1995) 979–990.
[8] M. Sudo, T. Tamaka, F. Saito, A study on development of leakage test apparatus, Conference Paper, Architecture Institute of Japan (AIJ) in Hokkaido, Paper No. 3021, 1995.
[9] D.T. Sheppard, K.W. Aittaniemi, Smoke leakage through class A boundaries, Underwriters Laboratories Report, No. CG-D-03-97, 1997.
[10] U. Kazuki, Fire testing of window glass for integrity and smoke leakage, Research Report, Architecture Institute of Japan (AIJ), Kanto branch, Paper No. 8, 1997.
[11] M. Sudo, T. Tamaka, T. Yoshikawa, K. Nakamura, Smoke leakage test of smoke proof fire shutter, Conference Paper, Architecture Institute of Japan (AIJ), Kyushu Branch, 1998.
[12] K. Aburano, T. Yamana, K. Wakamatsu, Smoke leakage tests of seat shutter, Conference Paper, Architecture Institute of Japan (AIJ), 2001.